JOURNAL OF MATERIALS SCIENCE **38** (2003) 1333– 1338

Effect of the surface oxide layer on transformation behavior and shape memory characteristics of Ti-Ni and Ti-Ni-Mo alloys

TAE-HYUN NAM, DAE-WON CHUNG, HEE-WOO LEE, JAE-HOON KIM, MI-SEON CHOI
Division of Materials Engineering and RIIT, Gyeongsang National University, Gazwa-dong 900, Chinju, Gyeongnam 660-701, Korea
E-mail: tahynam@nongac.gsnu.ac.kr

Oxidation behaviors of Ti-49Ni and Ti-48.3Ni-0.7Mo (at.%) alloys in dry air from 723 K to 1273 K have been investigated by means of scanning electron microscopy, energy dispersive X-ray spectroscopy and X-ray diffraction, and then effects of oxidation on transformation behavior and shape memory characteristics of the alloys were studied by means of differential scanning calorimetry and thermal cycling tests under constant load. Three-layered surface scale was formed in both alloys oxidized at temperatures higher than 1023 K, consisting of an outer TiO_2 layer, an intermediate layer of mixture of TiO_2 and Ni and an inner $TiNi_3$ layer. Thickness of the surface oxide layer increased from 1 μm to 50 μm with raising oxidation temperature from 923 K to 1273 K. The surface oxide layer raised transformation temperatures associated with the B2-B19′ and the R-B19′ transformation, while it did not almost change transformation temperatures associated with the B2-R transformation. Recoverable elongation was not changed in the alloys oxidized at temperatures below 823 K with raising oxidation temperature, whereas it decreased in the alloys oxidized at temperatures above 923 K. Transformation hysteresis was not almost changed by oxidation in a Ti-49Ni alloy, but it decreased largely in a Ti-48.3Ni-0.7Mo alloy.

1. Introduction

Ti-Ni based alloys are well known for their unique shape memory and pseudoelastic behaviors. In many applications of Ti-Ni based alloys, they are deformed to be wire and sheet forms. In order to obtain Ti-Ni alloy wire and sheet, their ingots are fabricated by casting, and then hot worked followed by cold working. Generally speaking, hot working is made at above 1023 K in air. In the process of cold working, they should be annealed at intermediate temperatures (673 K–873 K) because of their high strain hardening exponent, although they can be deformed in a ductile manner to about 50% strain prior to fracture [1].

Ti-Ni alloys have been known to react vigorously with oxygen to form oxide in air at elevated temperature. According to Chu *et al.* [2], the surface oxide of Ti-Ni alloys consisted of three layers which were an outer rutile layer, an inner $TiNi_3$ layer and intermediate layer consisting of a mixture of rutile and Ni(Ti). Activation energy for oxidation of Ti-Ni alloys was known to be 226–247 kJ/mol which is near that of pure Ti and was superior to that of low aluminium content Ti alloys [2, 3]. The thickness and structure of the oxide layer were also known to play an important role in the process of cold wire drawing [4, 5] and affect the pseudoelasticity of Ti-Ni alloys [6]. However, to the best of our knowledge, effect of the surface oxide layer on transformation behavior and shape memory characteristics of Ti-Ni alloys was not known well. The purpose of the present study are to investigate the oxidation behavior of Ti-Ni based alloys, and then to study effect of the surface oxide layer on transformation behavior and shape memory characteristics. Also oxidation effect on the shape memory characteristic of a Ti-48.3Ni-0.7Mo (at.%) alloy was investigated because it was known to be very suitable for medical application due to their good corrosion resistance [7].

2. Experimental procedure

Ti-49Ni and Ti-48.3Ni-0.7Mo (at.%) alloys were prepared by vacuum induction melting. From the previous study [8], a Ti-49Ni alloy was reported to transform in one-stage, i.e., the B2(cubic)-B19′ (monoclinic), while a Ti-48.3Ni-0.7Mo alloy was done to transform in two-stage, i.e., the B2-R(rhombohedral)-B19′. The alloy ingots were hot rolled at 1123 K to round bars with a diameter of 5 mm, and then cold drawn to wire with a diameter of 1.7 mm. All wire specimens were annealed at 1123 K for 3.6 ks in vacuum (1.33×10^{-3} Pa), and then quenched into iced water. After heat treatment, they were electropolished with an electrolyte

which consists of 95% CH_3COOH and 5% $HClO_4$ in volume.

Oxidation treatments were made in dry air at temperatures between 723 K and 1273 K for 0.6 ks. In order to investigate morphology and composition of oxide layers, scanning electron microscope(SEM) observations and energy dispersive X-ray spectroscopy (EDS) were made. X-ray diffraction experiments were made with Cu Kα radiation in order to investigate crystal structures of the oxide layer. Phase transformation behaviors of oxidized specimens were investigated by means of differential scanning calorimetry (DSC) with cooling and heating rate of 0.17 K/s. Shape memory characteristics of oxidized specimens were measured using thermal cycling tests under the constant load [9] with cooling and heating rate of 0.02 K/s.

3. Results and discussion

3.1. Oxidation behavior

Surface morphologies of oxidized Ti-49Ni and Ti-48.3Ni-0.7Mo alloys were investigated by SEM observations. Fig. 1 shows the results obtained from a Ti-48.3Ni-0.7Mo alloy. From X-ray diffraction which will be mentioned later, outer surface of oxidized specimens is known to be TiO_2 layer. With raising oxidation temperature from 923 K to 1273 K, it is found that TiO_2 layer is grown into pillar-like shape. Similar results were obtained from a Ti-49Ni alloy.

Fig. 2 shows cross-sectional SEM micrographs of an oxidized Ti-48.3Ni-0.7Mo alloy. Only one layer designated by A is seen in the specimen oxidized at 923 K as shown in Fig. 2a. The region designated by D is a Ti-Ni matrix. In specimens oxidized at the temperature higher than 1023 K, three layers designated by A, B and C are seen as shown in Fig. 2b, c and d, respectively. It is to be noted here that the B layer shows a lamellar structure consisting of B1 and B2 layers as shown in Fig. 2d. The compositions of A, B(B1, B2), C and D layers in Fig. 2d were measured by EDS, and then results obtained are shown in Table I. From Table I, it is found that Ti is a predominant element in A and B1 layers, while Ni is a predominant element in B2 layer. It is found also that the atomic ratio of Ti to Ni in C layer is roughly 1 to 3 and that the composition of D layer is near to that of the matrix.

In order to investigate crystal structures of A, B(B1, B2) and C layers in Fig. 2d, X-ray diffraction experiments were made with successively grinding the oxidized surface, and then results obtained are shown in Fig. 3. Fig. 3a is a diffraction pattern obtained before grinding. Diffraction peaks corresponding to TiO_2 are seen in the pattern. Fig. 3b is a diffraction pattern obtained after removing A layer completely. This means that the diffraction pattern of Fig. 3b is obtained from B layer. Diffraction peaks corresponding to TiO_2 and Ni are found. Fig. 3c is a diffraction pattern obtained after removing A and B layers. Diffraction peaks of TiNi(B2 parent phase) and $TiNi_3$ are found. From Figs 2, 3 and Table I, it is known that both A and B1 layer are TiO_2 and that B2 and C layer are Ni and $TiNi_3$, respectively. Similar results were reported by Chu *et al.* in an equiatomic TiNi alloy [2].

From Table I, B1 and B2 layers seem to contain a considerable amount of Ni and Ti, respectively, although they were known to be TiO_2 and Ni from Fig. 3. This may be attributed to the fact that the interlamellar spacing between B1 and B2 layer is less than 1 μm, and consequently an interference between B1 and B2 layer occurs during EDS. From Fig. 3c, diffraction peaks of

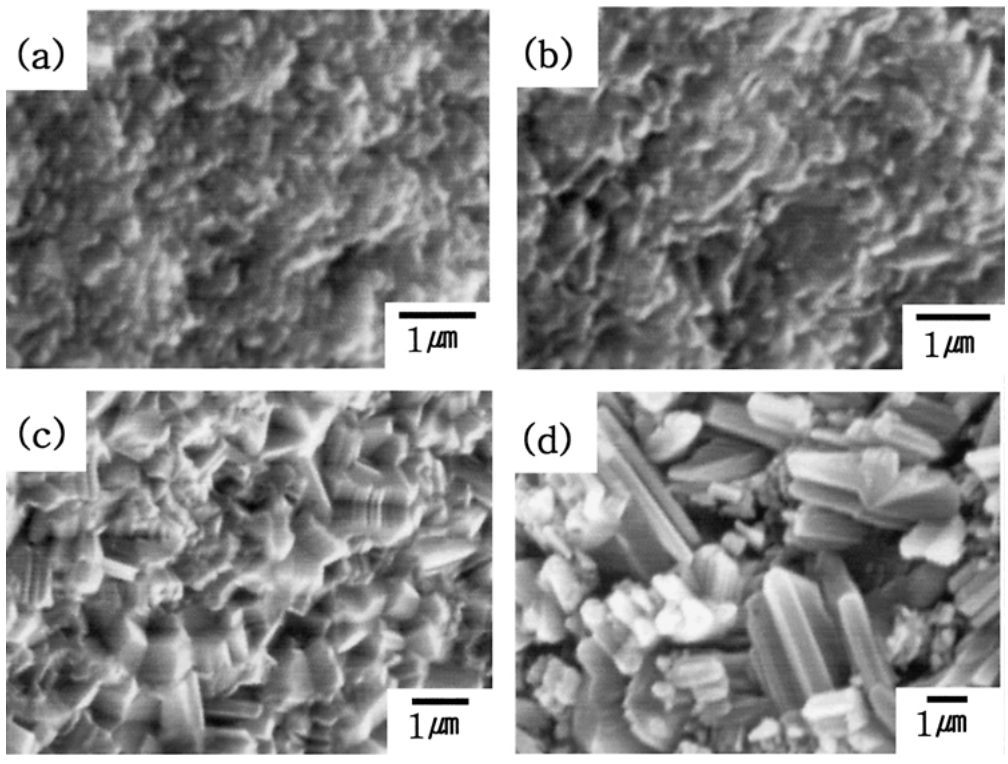

Figure 1 SEM micrographs of the surface of a 51Ti-48.3Ni-0.7Mo alloy oxidized at (a) 923 K, (b) 1023 K, (c) 1123 K and (d) 1273 K.

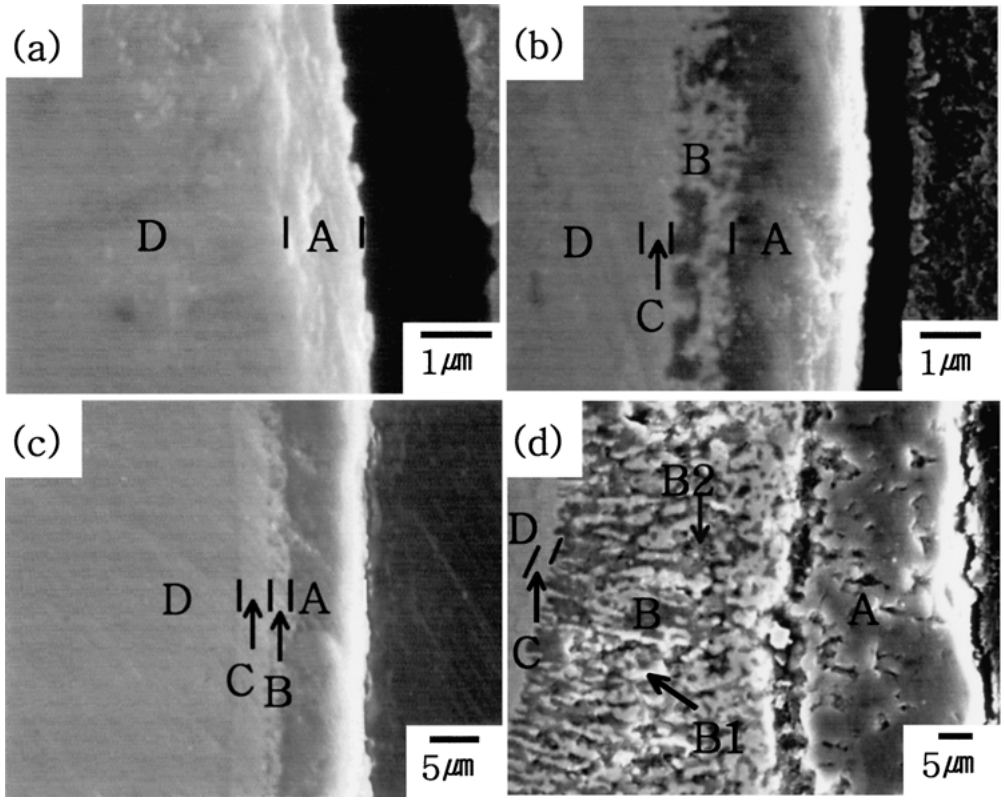

Figure 2 SEM micrographs of cross sections of a 51Ti-48.3Ni-0.7Mo alloy oxidized at (a) 923 K, (b) 1023 K, (c) 1123 K and (d) 1273 K.

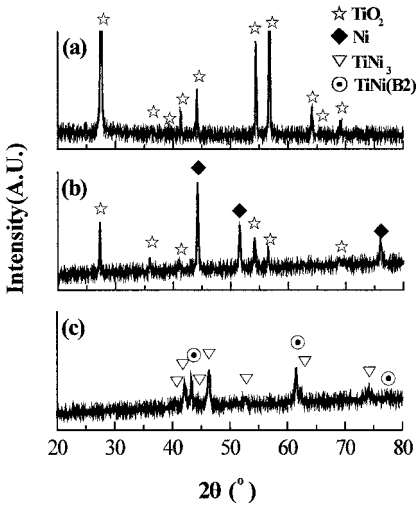

Figure 3 X-ray diffraction patterns of a 51Ti-48.3Ni-0.7Mo alloy oxidized at 1273 K, (b) was obtained after removing A layer in Fig. 2d and c was obtained after removing A and B layer in Fig. 2d.

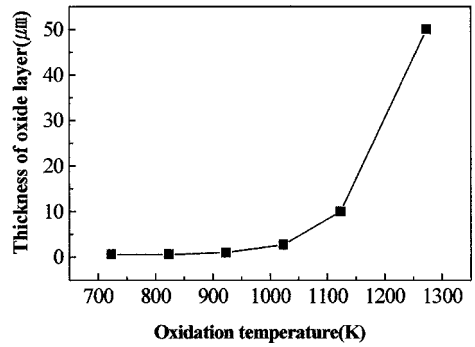

Figure 4 The relationship between oxidation temperatures and thickness of oxide layer.

TiNi matrix were found, although layer C was known to be $TiNi_3$. This may be ascribed to the fact that the thickness of C layer is so thin (about 2 μm) that X-ray possibly pass through C layer, and that diffraction from D matrix region occurs.

From Fig. 2, the thickness of oxide layer (A + B + C) was measured, and then plotted against oxidation temperatures in Fig. 4. Thickness of the oxide layer is very thin less than 1 μm at oxidation temperatures below 923 K, while it increases abruptly with raising oxidation temperature above 1023 K.

TABLE I Chemical compositions of oxide layers in Fig. 2d

Region	A	B1	B2	C	D
Ti	97.8	88.8	12.8	26.5	48.2
Ni	2.2	11.2	87.2	73.5	51.8

Fig. 5 shows X-ray diffraction patterns of a Ti-48.3Ni-0.7Mo alloy before and after oxidation at 823 K, 923 K, 1023 K, 1123 K, respectively. Before oxidation, as shown in Fig. 5a, diffraction peaks corresponding to the R phase are found. After oxidation at 823 K, however, diffraction peaks of the R phase disappear and those of the B2 and TiO_2 are found, as shown in Fig. 5b. This is attributed to the fact that the B2-R transformation start temperature, T_R decreases due to the decrease in Ti content of the matrix around TiO_2. Martensitic transformation temperatures of Ti-Ni based alloys were known to decrease with decreasing Ti content [10, 11]. With raising oxidation temperature from 823 K to 1123 K, intensity of diffraction peaks of TiO_2 increases largely. Diffraction peaks corresponding to

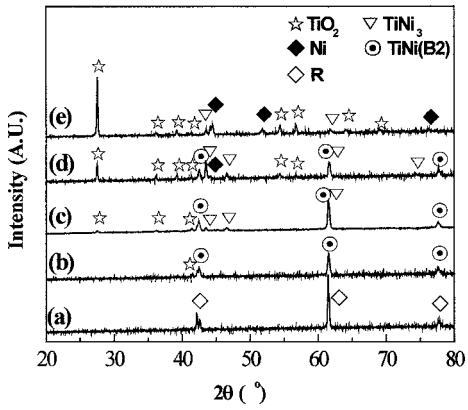

Figure 5 X-ray diffraction patterns of a 51Ti-48.3Ni-0.7Mo alloy oxidized at various temperatures, (a) before oxidation, (b) 823 K, (c) 923 K, (d) 1023 K and (e) 1123 K.

$TiNi_3$ phase are found at the specimens oxidized at above 923 K, and those corresponding to Ni are found at the specimens oxidized at above 1023 K.

Comparing Fig. 5c and d, it is found that intensity of diffraction peaks corresponding to TiO_2 and $TiNi_3$ increases simultaneously with raising oxidation temperature from 923 K to 1023 K. This result strongly suggests that formation of $TiNi_3$ phase is related with the formation of TiO_2. With increasing the amount of TiO_2, Ti content of the matrix is expected to decrease, and consequently the $TiNi_3$ phase is formed. Comparing Fig. 5d and e, it is found that intensity of diffraction peaks of Ni increases with raising oxidation temperature from 1023 K to 1123 K, while that of $TiNi_3$ phase decreases. This means that Ni is formed by decomposition of $TiNi_3$ phase. Similar oxidation behavior was observed in a Ti-49Ni alloy.

3.2. Phase transformation behavior

In order to investigate the effect of oxidation on phase transformation behavior, DSC measurements were made on oxidized specimens, and then results obtained are shown in Figs 6 and 7. Fig. 6 shows DSC curves of a Ti-49Ni alloy oxidized at various temperatures. From Fig. 6, DSC peaks corresponding to the B2-B19′ transformation on cooling curves and those corresponding to the B19′-B2 transformation on heating curves are found, irrespective of oxidation temperatures. The B2-B19′ transformation start temperature (M_s) and the B19′-B2 reverse transformation finish temperature (A_f) were determined by a tangential extrapolation method [12]. Fig. 7 shows DSC curves of a Ti-48.3Ni-0.7Mo alloy oxidized at various temperatures. Two DSC peaks designated by R and M are found on cooling curves at all oxidation temperatures. The peak designated by R is due to the B2-R transformation and that designated by M is due to the R-B19′ transformation. It is to be noted here that a temperature gap between the two DSC peaks decreases with raising oxidation temperature. On heating curves, two DSC peaks designated by M* and R* appear in specimens oxidized below 923 K. The DSC peak designated by M* is ascribed to the B19′-R transformation and that designated by R* is done to the R-B2 transformation.

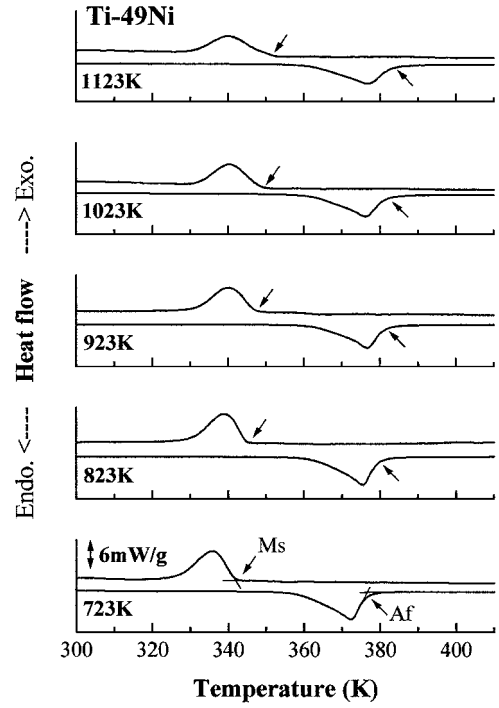

Figure 6 DSC curves of a 51Ti-49Ni alloy oxidized at various temperatures.

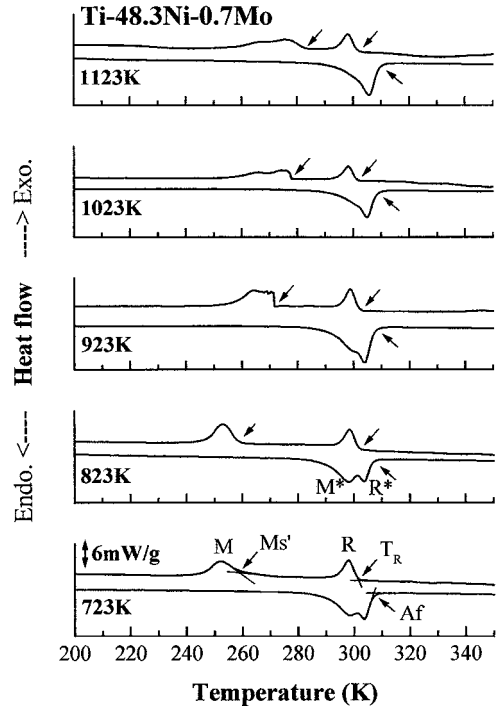

Figure 7 DSC curves of a 51Ti-48.3Ni-0.7Mo alloy oxidized at various temperatures.

However, only one DSC peak appears in specimens oxidized above 1023 K. This means that the B19′-R and the R-B2 transformation are not separated clearly in specimens oxidized above 1023 K. The B2-R transformation start temperature (T_R), the R-B19′ transformation start temperature (M_s') and the R-B2 or the B19′-B2 transformation finish temperature (A_f) are determined by the extrapolation method as shown in Fig. 7.

From Figs 6 and 7 measured transformation temperatures were, plotted against oxidation temperatures as

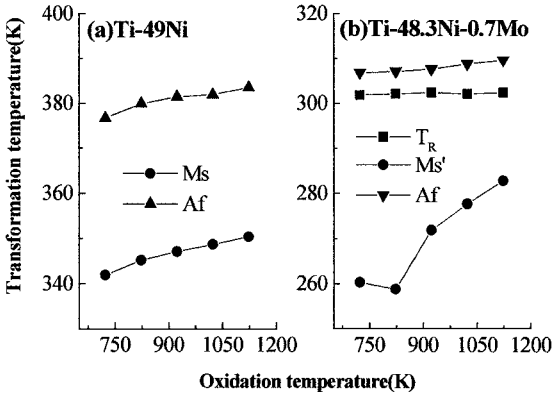

Figure 8 The relationship between oxidation temperatures and transformation temperatures.

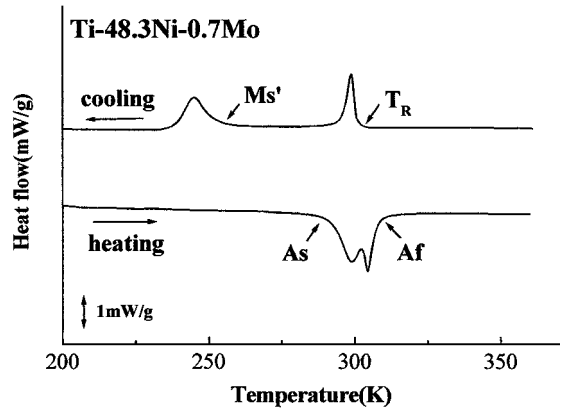

Figure 9 DSC curves of a 51Ti-48.3Ni-0.7Mo alloy obtained after removing the surface oxide layer completely.

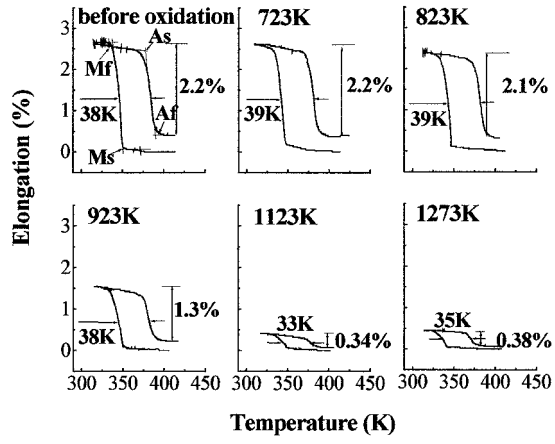

Figure 10 Temperature-elongation curves of a 51Ti-49Ni alloy oxidized at various temperatures.

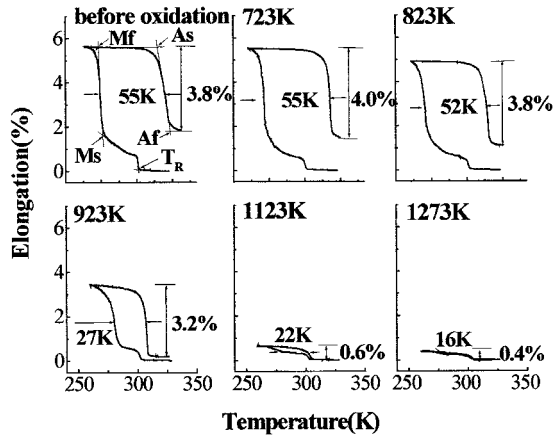

Figure 11 Temperature-elongation curves of a 51Ti-48.3Ni-0.7Mo alloy oxidized at various.

shown in Fig. 8. With raising oxidation temperature, M_s and A_f are found to increase in a Ti-49Ni alloy as shown in Fig. 8a. In a Ti-48.3Ni-0.7Mo alloy, however, T_R, and A_f are found to be almost kept constant with raising oxidation temperature, as shown in Fig. 8b, although M_s', increases. The small increase in A_f above 1023 K may be ascribed to the fact that the B19′-R and the R-B2 transformations are not separated clearly at oxidation temperatures above 1023 K. This means that an oxidation affect largely transformation temperatures associated with the B2-B19′ and the R-B19′ transformations, while it almost dose not affect those associated with the B2-R transformation.

It is well known fact that volume of Ti-Ni alloys contract during the B2-B19′ and B2-R transformation [13]. Therefore, transformation temperatures of Ti-Ni alloys were reported to increase by applying hydrostatic pressure [14, 15]. When Ti-Ni alloys are oxidized, the oxide layer formed at the surface is thought to impose a compressive stress to specimens because molar volume of a Ti-Ni alloy increases by oxidation [16]. Therefore, the increase in transformation temperatures with raising oxidation temperature in Fig. 8 is attributed to a compressive stress induced by the oxide layer. As mentioned before, however, transformation temperatures associated with the B2-R transformation are almost kept constant. This is ascribed to the fact that the volume change associated with the B2-R transformation (−0.013%) is very small comparing with that associated with the B2-B19′ transformation (−0.526%) [13].

Fig. 9 shows DSC curves of a Ti-48.3Ni-0.7Mo alloys obtained after removing completely the surface oxide layer formed by oxidation at 1123 K, respectively. As shown in the figure, T_R, M_s' and A_f in a Ti-48.3Ni-0.7Mo alloy are found to be 301 K, 240 K and 308 K, respectively. Comparing Fig. 9 with Fig. 7, it is found that M_s' in a Ti-48.3Ni-0.7Mo alloy decrease by removing the surface oxide layer, while T_R and A_f in a Ti-48.3Ni-0.7Mo alloy are not almost changed.

3.3. Shape memory characteristics

Figs 10 and 11 are elongation vs. temperature curves of oxidized Ti-49Ni and Ti-48.3Ni-0.7Mo alloys, respectively. All curves were obtained under the applied stress of 60 Mpa. In Fig. 10, the abrupt elongation which starts to occur at M_s is due to the B2-B19′ transformation and recovery of the elongation which stars to occur at A_s is due to the B19′-B2 transformation. Before oxidation, transformation hysteresis (ΔT) is found to be 38 K. After oxidation, it is almost kept constant (35 K) with raising oxidation temperature from 723 K to 1273 K. This is originated from the fact that M_s and A_f increased with raising oxidation temperature as shown is Fig. 8a. Before oxidation, the recoverable elongation (ε_R) is found to be 2.2%. After oxidation, it is almost kept constant in the specimens oxidized

below 823 K. However, it decreases from 2.1% to 0.3% with raising oxidation temperature from 823 K to 1273 K.

In Fig. 11, a relatively small elongation which starts to occur at T_R is due to the B2-R transformation and a relatively large elongation which starts to occur at M_s is due to the R-B19′ transformation. Recovery of the elongation which stars to occur at A_s is due to the B19′-B2 transformation. Before oxidation, transformation hysteresis (ΔT) is found to be 55 K. After oxidation, it is almost kept constant in the specimens oxidized below 823 K. However, it decreases from 52 K to 16 K with raising oxidation temperature from 823 K to 1273 K. This is ascribed to the fact that M_s increased with raising oxidation temperature, while A_f was almost kept constant as shown in Fig. 8b. Before oxidation, the recoverable elongation (ε_R) is found to be 3.8%. After oxidation, it is almost kept constant in the specimens oxidized below 823 K. However, it decreases from 3.8% to 0.4% with raising oxidation temperature from 823 K to 1273 K.

From Figs 10 and 11, it was found that ε_R started to decrease largely when oxidation temperature is higher than 923 K. From Fig. 4, it was found that thickness of oxide layers started to increase largely at 923 K. Therefore, it is thought that the large decrease in ε_R which start to occur at 923 K is related to the large increase in thickness of oxide layers. In order to prevent from decreasing ε_R by oxidation, heat treatment temperatures should be below 923 K.

4. Conclusions

1. The surface oxide layer of Ti-49Ni and Ti-48.3Ni-0.7Mo alloys oxidized at temperatures higher than 1023 K consisted of an outer TiO_2 layer, an intermediate layer of mixture of TiO_2 and Ni and an inner $TiNi_3$ layer.

2. Thickness of the surface oxide layer increased from 1 μm to 50 μm with raising oxidation temperature from 923 K to 1273 K.

3. Transformation temperatures associated with the B2-B19′ and the R-B19′ transformation rose by oxidation, while those associated with the B2-R transformation did not change.

4. Recoverable elongation was not almost changed in the alloys oxidized at temperatures below 823 K with raising oxidation temperature, whereas it decreased in those oxidized at temperatures above 923 K.

5. Transformation hysteresis was not almost changed by oxidation in a Ti-49Ni alloy, but it decreased largely in a Ti-48.3Ni-0.7Mo alloy.

Acknowledgement

This work was supported by Korea Energy Management Corporation temperatures.

References

1. S. MIYAZAKI, K. OTSUKA and Y. SUZUKI, *Scripta Metall.* **15** (1987) 287.
2. C. L. CHU, S. K. WU and Y. C. YEN, *Mater. Sci. Eng.* A **216** (1996) 193.
3. T. SATO, T. ISANO and T. HONMA, *J. Jpn. Inst. Met.* **38** (1974) 242 (in Japanese).
4. S. K. WU, H. C. LIN and Y. C. YEN, *Mater. Sci.* (2001) in press.
5. T. H. NAM, D. W. CHUNG, J. P. NOH and H. W. LEE, *J. Mater. Sci.* **36** (2001) 418.
6. H. C. LIN, S. K. WU and Y. C. YEN, in Proceedings of the 2nd Pacific Rim International Conference on Advanced Materials and Processing, Kyongju, June 1995, edited by K. S. Shin *et al*. (The Korean Institute of Metals and Materials, 1995) p. 1167.
7. V. E. GUNTER, "Medical Materials and Implant with Shape Memory Effect," (1998) In Russian.
8. T. H. NAM, D. W. CHUNG, J. S. KIM and S. B. KANG, *Mater. Lett.* **52** (2002) 234.
9. T. H. NAM, T. SABURI, Y. KAWAMURA and K. SHIMIZU, *Mat. Trans. JIM* **31** (1990) 26.
10. J. E. HANLON, S. R. BUTLER and R. J. WASILEWSKI, *Trans. Metall. Soc. AIME* **239** (1967) 1323.
11. A. GYOBU, Y. KAWAMURA, H. HORIKAWA and T. SABURI, *Mat. Trans. JIM* **37** (1996) 697.
12. J. KWARCIAK and H. MORAWIEC, *J. Mater. Sci.* **23** (1988) 551.
13. C. M. WAYMAN, in Proceedings of the International Conference on Martensitic Transformations, NARA, 1986, edited by K. Shimizu *et al.* (The Japan Institute of Metals, 1986) p. 645.
14. T. KAKESHITA, K. SHIMIZU, S. NAKAMICHI, R. TANAKA and S. ENDO, *Mat. Trans. JIM* **33** (1882) 1.
15. V. A. CHERNENKO, O. M. BABII, V. V. KOKOLIN, A. I. LOTKOV and V. N GRISHKOV, *Phys. Met. Metall.* **81** (1996) 549.
16. S. K. WU and C. M. WAYMAN, *Acta Metall.* **36** (1988) 1005.

Received 13 November 2001
and accepted 25 November 2002